Proceedings of ASME 2020 39th International Conference on Ocean, Offshore and Arctic Engineering
OMAE2020
June 28–July 3, Fort Lauderdale, FL, USA

OMAE2020-19039

A SENSITIVITY STUDY OF VESSEL HYDRODYNAMIC MODEL PARAMETERS

Xu Han[1], Svein Sævik, Bernt Johan Leira
NTNU
Trondheim, Norway

ABSTRACT

In the recent decade, maritime and energy industries have realized the potential of using operational data in combination with a virtual replication of the real physical asset, termed the digital twin. The digital twin then serves as a platform for data management, asset monitoring, and inspection and maintenance management, featuring an improved basis for cost effective operations and future decision making in terms of e.g. life extension. The present paper deals with application of the digital twin concept in marine operations where it is essential to handle the inherent uncertainties of vessel performance by applying a model that can adapt to the real operating conditions. In this paper a case study is presented for identifying the most sensitive parameters in the vessel hydrodynamic model w.r.t. the vessel motion RAOs. The study also shows that the parametric sensitivity depends on the interesting vessel response parameter, wave direction and loading condition. A digital twin adaptive to various operational conditions may require parametric tuning of the numerical model. It is important to identify the correct parameter(s) for modification. A simplified and idealized case study is also carried out to test the requirements to a successful parameter identification for model tuning.

NOMENCLATURE

A_{P90}^{loc}	The P90 value of heave acceleration at the "loc" location, for a certain sea state
$A(\omega)$	Added mass coefficient
B	Vessel breadth
C_{ij}	Restoring stiffness to i[th] dof due to motion in j[th] dof
COG	Center of Gravity
D	Vessel draft
dof	Degree of freedom, 1 – Surge, 2 – sway, 3 – heave, 4 – roll, 5 – pitch, 6 – yaw
$F(\omega, u\|\beta_w)$	Excitation force from waves, on complex form, including Froude-Krylov and diffraction forces
GMT	Transverse metacentric height
GML	Longitudinal metacentric height
g	Gravity
H	water depth
H_S	Significant wave height
I_{xx}	moment of inertia w.r.t. vessel x-axis
I_{yy}	moment of inertia w.r.t. vessel y-axis
I_{zz}	moment of inertia w.r.t. vessel z-axis
k	Wave number
L_{PP}	Length between perpendiculars
loc	Location
M	Mass of vessel
MRU	Motion Reference Unit
OSV	Offshore Supply Vessel
RAO	Response Amplification Operator
SS	Sea state
T	Wave period
T_Z	Zero-upcrossing wave period
u	Vessel speed
Var	Variable, the parameter for sensitivity study
V_{P90}^{loc}	The P90 value of heave velocity at the "loc" location, for a certain sea state
w.r.t.	with respect to
XCG	longitudinal coordinate of vessel COG

[1] Contact author: xu.han@ntnu.no

YCG	transverse coordinate of vessel COG
ZCG	vertical coordinate of vessel COG
β_{ij}	The linear damping to the i[th] dof due to motion in j[th] dof, $\beta_{ij} = {\beta_{ij}}^{p} + {\beta_{ij}}^{a}$
${\beta_{ij}}^{p}$	Potential theory related damping
${\beta_{ij}}^{a}$	linearized damping in addition to the potential theory related damping term ${\beta_{ij}}^{a} = \xi \cdot \beta_{ij,cr}$
$\beta_{ij,cr}$	Critical damping, $\overline{\overline{\beta_{cr}}} = 2\sqrt{(\bar{\bar{A}}(\omega) + \bar{\bar{M}}) \cdot \bar{\bar{C}}}$
β_w	Wave direction w.r.t. vessel coordinate system
ω	Wave frequency
ω_e	Encounter frequency
λ	Wave length
ζ_a	Wave amplitude
ϕ_a	Wave slope amplitude $\phi_a = k \cdot \zeta_a$

INTRODUCTION

Industrial practice on vessel seakeeping analyses has been well standardized due to the developed theory of ocean waves and vessel hydrodynamics during the last century, see e.g., [1]. The theory and practice of modelling ocean waves and structural hydrodynamics is usually simplified and sometimes linearized. For example, the vessel response to ocean waves is very often simply represented in frequency domain by linear transfer functions (i.e. RAO) in 6 dof's. As a supplement, model tests in laboratory and virtual tests play an important role in the design phase when determining the hydrodynamic coefficients of vessels.

The numerical model developed in design phase can be extended to a digital twin of the real physical asset, supporting monitoring, maintenance, real-time decision making, remote control, automation etc. related to operations. Hundreds of sensors are installed in a typical offshore vessel. With developed technologies on sensors, data management, and remote communication, industries and researchers have started to explore different applications of the digital twin concept. Among them, onboard decision support systems (ODSS) have been a very promising application, aiming at real-time reliable prediction of critical responses.

Many ODSS for marine and offshore activities have been developed during the last decade, ref. [2], [3], [4], [5], [6], [7], [8], [9], mainly focusing on technologies providing more accurate wave prediction, in forms of either wave surface elevations or wave spectra. Linear transfer function between wave and vessel motion (i.e. RAO) has been applied in most ODSSs. The influences from the uncertainties of RAO have been studied, e.g., [10], [11], [12]. Challenges on insufficient accuracy of roll motion prediction by using RAO, is commonly observed, due to the highly nonlinear damping effect [13].

Sensor data with acceptable quality could be used to reduce the uncertainties and conservatism of the prediction through active modification of the numerical vessel hydrodynamic model. This has a huge commercial benefit regarding safety and reliability improvement, and potential cost reduction.

However, there are hundreds of parameters that can be varied in one hydrodynamic model, and normally very little prior knowledge is available on which parameters should be selected to modify. Considering measurement noises, information discretization, and uncertainties from model simplification, vessel hydrodynamic model tuning could be very challenging.

The work described in this paper, is based on a parametric sensitivity study of one OSV to identify which parameters that govern the vessel response to ocean waves in terms of RAOs, and to study the possibility of identifying the right parameters to tune based on acquired measurement data.

The paper is organized as follows. The basis of the vessel numerical hydrodynamic model is described in section "Case Study Basis". In section "Theory", the basic theories on linear dynamic systems in the frequency domain, wave dispersion and kinematics are briefly described. Then, the parametric sensitivity studies on water depth, vessel speed, inertia terms, metacentric heights and additional damping terms are reported in more detail in the section "Parametric Sensitivity Study", where the important parameters are identified. Afterwards, a simple case study is presented in section "Parameter Identification", aiming to identify the right tuning parameters. Then, some key findings and challenges are summarized in section "Conclusion and Discussion".

CASE STUDY BASIS

The case study was based on the hydrodynamic model for one OSV. The primary information of the vessel is summarized in Table 1. The coordinates refer to the reference coordinate system moving steadily at the vessel forward speed where the positive x-axis points from stern to bow (x=0 aft), the z-axis is pointing vertically upward from keel (z=0 at keel) and the y-axis is normal to the x-z plane where y=0 is at the longitudinal symmetric plane. Wave direction (heading) follows the same coordinate system, i.e. for waves at 0 heading propagates along the positive x-axis.

To investigate the sensitivity of hydrodynamic model parameters w.r.t. the vessel motion RAOs, both ballast and full loading conditions with infinite water depth were selected as base case. The base cases also included 0.5m GMT correction due to free surface effect and an addition roll damping (${\beta_{44}}^{a} = 5\% \cdot \beta_{44,cr}$). Only surge, sway, heave, roll and pitch amplitudes were considered, i.e. the influence on RAO phase angles were not included. The RAOs were calculated at the MRU location midship, approximately (60m,0m,11m).

The variables listed in Table 2 were included in the sensitivity studies. The ranges of water depth (H) and vessel speed (u) represented the normal operation conditions, while the ranges of the other variables reflected parametric uncertainties with prior knowledge of the operational conditions. The parameter variations were based on engineering judgement as the ranges can depend on many factors, such as the sensor accuracy, operational conditions, vessel type and vessel geometry.

Table 1: Vessel information, base cases

Parameters	Value	Unit
L_{PP}	~120	m
B	~27	m
D (Ballast)	~5.1	m
D (Full)	~6.8	m

Table 2: Studied variables

Variable	Range RAO visual inspection	Range numerical comparison
H*	20 – 2000 m	
u*	0 – 20 knots	
XCG	$\pm 4m$	$\pm 4m$
YCG	$\pm 1m$	$\pm 1m$
ZCG	$\pm 1m$	$\pm 1m$
M	$\pm 10\%$	$\pm 10\%$
I_{xx}	$\pm 10\%$	$\pm 10\%$
I_{yy}	$\pm 10\%$	$\pm 10\%$
I_{zz}	$\pm 10\%$	$\pm 10\%$
GMT	$\pm$1.5m	$\pm$0.5m
GML*	$\pm$10 m	
${\beta_{11}}^{a}$ *	0 - 16% of $\beta_{11,cr}$	
${\beta_{22}}^{a}$ *	0 - 16% of $\beta_{22,cr}$	
${\beta_{33}}^{a}$	0 - 16% of $\beta_{33,cr}$	2 – 14%
${\beta_{44}}^{a}$	2 - 16% of $\beta_{44,cr}$	2 – 14%
${\beta_{55}}^{a}$ *	0 - 16% of $\beta_{55,cr}$	

*Parameters excluded for numerical comparison of sensitivity studies. Reasons are explained in sections "Metacentric height", "Additional damping" and "Numerical results".

THEORY

Frequency domain vessel motion RAOs can be calculated based on the equation of motion:

$$\left(\bar{\bar{A}}(\omega_e) + \bar{\bar{M}}\right)\ddot{\vec{x}} + \bar{\bar{\beta}}(\omega_e)\dot{\vec{x}} + C\vec{x} = \vec{F}(\omega, u|\beta_w) \quad (1)$$

$$RAO(\omega, u|\beta_w) = \frac{\vec{F}(\omega, u|\beta_w)}{-{\omega_e}^2\left(\bar{\bar{A}}(\omega_e) + \bar{\bar{M}}\right) + i\omega_e\bar{\bar{\beta}}(\omega_e) + \bar{\bar{C}}} = \bar{\bar{D}}(\omega_e) \cdot \vec{F}(\omega, u|\beta_w) \quad (2)$$

As a result, RAOs are complex-valued operators. The hydrodynamic coefficients and excitation forces were calculated by commercial software Wasim contained in the Sesam program package [14]. Wasim is a 3D time-domain hydrodynamic analysis software by Rankine panel method [15]. Luo [16] summarizes the common assumptions, boundary conditions and governing equations leading to the linear potential theory applied in Wasim. Each Wasim analysis was run for one wave period and operation condition where the "operation condition" herein is defined by vessel heading, loading condition, and vessel speed. The outputs of Wasim analyses from all wave periods are transferred to frequency domain. The database of hydrodynamic coefficients and excitation forces were therefore obtained for each operating condition and applied to generate the vessel motion RAO for each specific operation condition, based on formula (2).

For a valuable comparison, the quality of hydrodynamic coefficient calculation and RAO calculation should be assured. It is essential to make sure that the RAO peak is captured by having a sufficient number of hydrodynamic calculations around the peak period; that the time step applied for numerical simulation (time domain) is sufficiently small; and that the number of panels is sufficient, ref. [14].

Wave dispersion

The wave dispersion, referring to [1], can normally be expressed by:

$$\omega^2 = g \cdot k \cdot tanh(k \cdot H) \quad (3)$$

k is the wave number, $k = \frac{2\pi}{\lambda}$. So, the dispersion relation could also be written as:

$$\lambda = \frac{g}{2\pi}T^2 \tanh(2\pi\frac{H}{\lambda}) \quad (4)$$

It shows that the wave length, wave number and wave slope amplitude ($k\zeta_a$) are influenced by wave period and water depth.

Water particle motion

For linear potential wave theory, both the horizontal and vertical water particle velocity are dependent on water depth.

$$u = \omega a \cdot \frac{\cosh \mathrm{k}(z+H)}{\sinh kd} \cdot \sin(\omega t - kx) \quad (5)$$

$$w = \omega a \cdot \frac{\sinh \mathrm{k}(z+H)}{\sinh kd} \cdot \cos(\omega t - kx) \quad (6)$$

But at sea surface, the vertical velocity is independent of water depth:

$$u = \omega a \cdot \frac{\cosh k \cdot H}{\sinh k \cdot H} \cdot \sin(\omega t - kx) \quad (7)$$

$$w = \omega a \cdot \cos(\omega t - kx) \quad (8)$$

Therefore, as shown in Figure 1, the water particle trajectory is influenced by water depth and wave period. Larger wave period amplifies the water depth effect on the water particle horizontal motion.

Encounter frequency of advancing vessel

The vessel with forward speed experiences wave loads in encounter frequency instead of wave frequency. The encounter frequency is expressed:

$$\omega_e = |\omega - k \cdot u \cdot cos\beta_w| \quad (9)$$

For following wave conditions, i.e., $\beta_w = [0°, 90°)$, the term inside of absolute operator can be negative. This leads to a so-called 3-to-1 mapping problem between wave frequency and encounter frequency for following waves [17]. Therefore, for

simplification, this paper only considers head waves, $\beta_w = [90°, 180°]$.

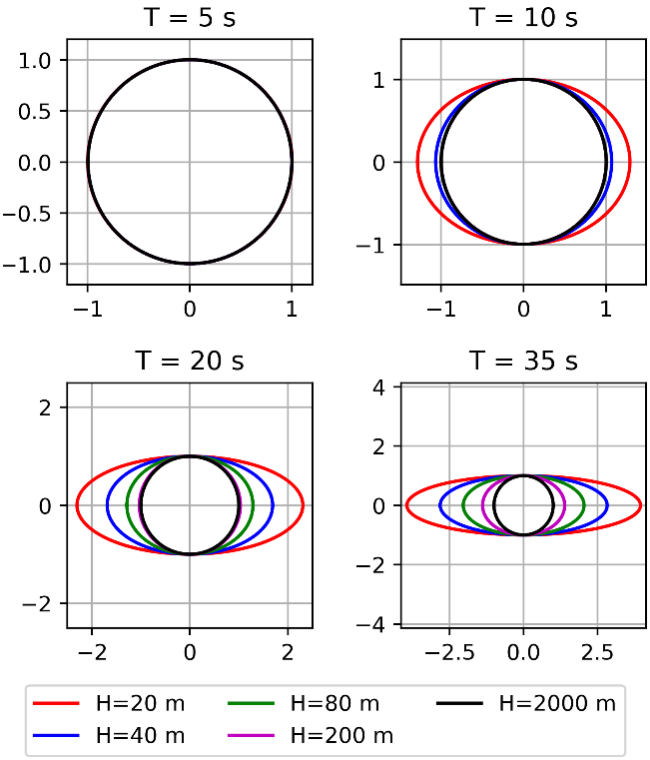

Figure 1: Trajectories of water particles, $\zeta_a = 1$

PARAMETRIC SENSITIVITY STUDY

Water depth

From equations (4) (7) and (9), the water depth influences the wave number k (Figure 2), and consequently the wave kinematics at sea surface and along water depth, wave length (and wave slope), and encounter frequency for advancing vessel. From Figure 3, the pitch RAO sensitivity to water depth shows a shift of the peak period for shallow water. This could be the effect of water depth on wave length (and wave steepness), which is also observed in [18]. Figure 4 shows that the excitation force on pitch is influenced by water depth on large wave periods due to its effect on wave steepness (shown in Figure 2). In addition to the water steepness influence on excitation force, the RAO peak amplitude also highly depends on the added mass and damping coefficients which are influenced by encounter frequency and wave kinematics on vessel wet body (e.g. Figure 5). Consequently, they are all influenced by water depth. In Figure 3, pitch RAOs at no forward speed was selected, intending to tell the shift of peak period is due to the water depth effects on λ (ϕ_a) and wave kinematics, instead of ω_e. For $u = 0kn$, $\omega_e = \omega$. Figure 6 shows that translational motion RAO amplitude does not converge at large periods when considering water depth effect on the horizontal water particle motion.

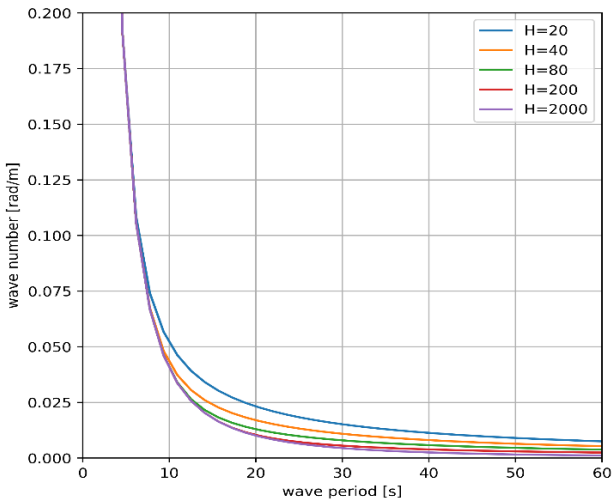

Figure 2: Wave number (k) influenced by wave period and water depth [m].

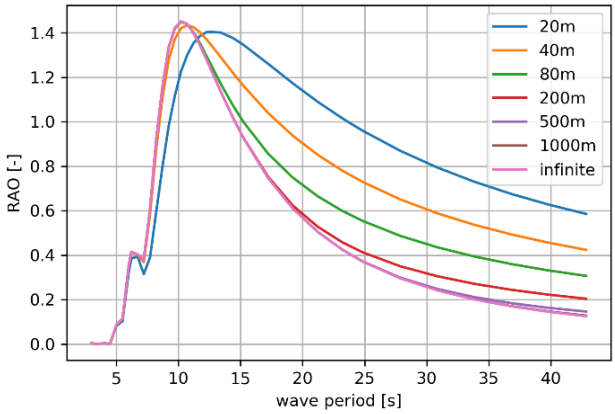

Figure 3: Pitch RAO for water depth sensitivity, ballast condition at 180° heading, with no forward speed.

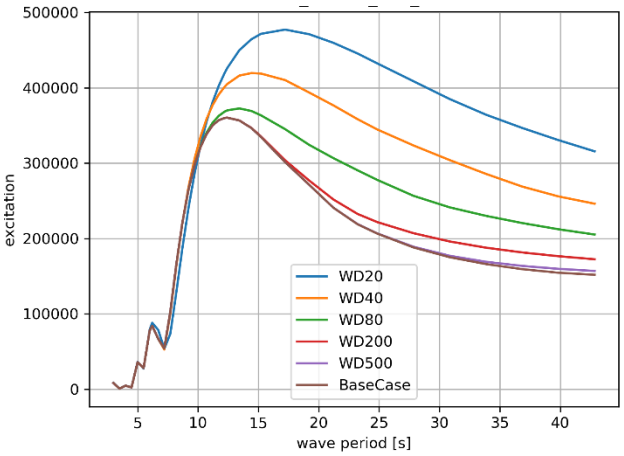

Figure 4: Pitch excitation moment for water depth sensitivity, ballast condition at 180° heading, with no forward speed. "WD" in legend means water depth [m].

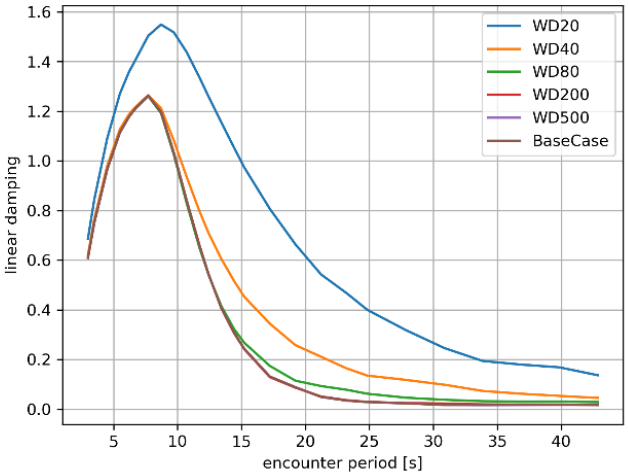

Figure 5: Damping on pitch for water depth sensitivity, ballast condition at 180° heading, with no forward speed. "WD" in legend means water depth [m].

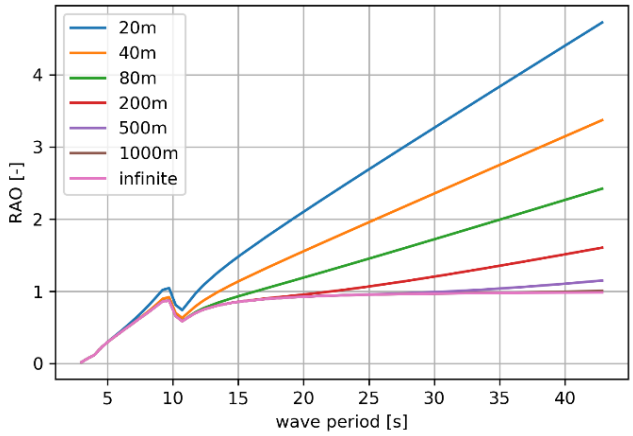

Figure 6: Sway RAO for water depth sensitivity, ballast condition at 90° heading, 10kn speed.

Vessel speed

The influence of vessel forward speed on vessel response is complex. For examples, Faltinsen [1] and MacTaggart [19] tried to show how the vessel speed can affect vessel motions. Simply speaking, vessel speed significantly affects the hydrodynamic coefficients, response period, total velocity potential and free surface conditions (i.e., kinematic and dynamic pressure) in the vessel moving reference system. Consequently, both diffraction and radiation are affected. The Froude-Krylov force is not dependent on speed but is oscillated with the encounter frequency.

Both $\overline{\overline{D}}(\omega_e)$ (free vibration) and $\vec{F}(\omega, u|\beta_w)$ (incident and wave diffraction loads) can possibly govern the peaks in RAO amplitudes (local and global peaks). For $\overline{\overline{D}}(\omega_e)$ term governed peaks (e.g. the peak at about 10s in Figure 7), the peak period usually locks to the encounter period. For $\vec{F}(\omega, u|\beta_w)$ term governed peaks (e.g. the peak at about 4s in Figure 7), the peak period usually links (but not strictly locks) to the wave period. Vessel speed influences the kinematic and dynamic pressure boundary conditions on surface, and consequently influences both the peak amplitude and peak period of the wave and vessel speed induced loads (i.e., $\vec{F}(\omega, u|\beta_w)$). When the peaks of $\overline{\overline{D}}(\omega_e)$ and $\vec{F}(\omega, u|\beta_w)$ are close, the peak could be located at any period in between.

In this case study, higher speed leads to smaller peak amplitude for roll RAO and its coupled sway RAO and larger peak amplitude for pitch RAO and its couple heave RAO, which were also observed in lecture notes [20].

Inertia terms

Inertia terms XCG, YCG, ZCG, M(D), I_{xx}, I_{yy} and I_{zz} were studied. In practice, those parameters vary from operation to operation and includes considerable uncertainty. Varying COG will change trim, heel, waterline and wet body surface. Varying moment of inertias will influence RAO for the corresponding rotational dof, and the coupled translational dof. Varying mass will change draft and consequently change the waterline and wet body surface. These will lead to any possible changes on RAOs, depending on hull geometry and mass distribution.

The case study shows that inertia terms can significantly influence the RAO amplitudes for a wide range of wave periods around the peak period. In addition, the RAO resonance period can also be influenced by inertia terms (e.g., moments of inertia). Roll and sway are sensitive to all of the studied relevant inertia terms, while pitch and heave are only sensitive to some of them. Studies show that the heave RAO at MRU is sensitive to XCG and M whereas pitch RAO at MRU is sensitive to XCG and I_{yy}.

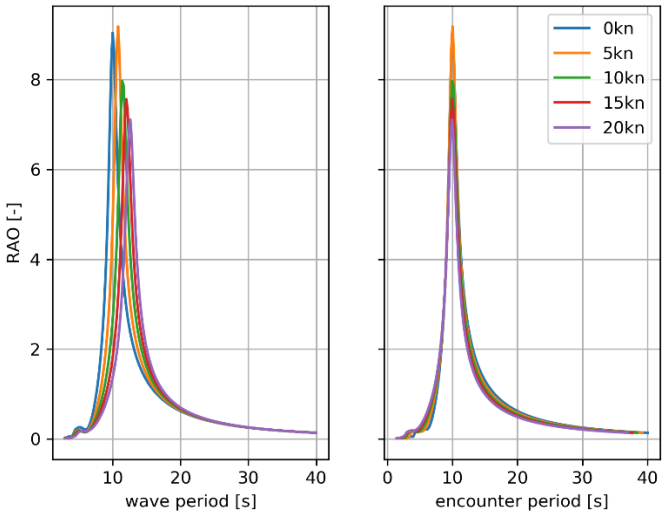

Figure 7: Roll RAO for vessel speed sensitivity, ballast condition at 120° heading.

Metacentric height

Metacentric heights GMT and GML directly determine the restoring moments for roll and pitch motions, as shown in equation (10). Variation of vessel inertia distribution will naturally lead to variation of metacentric heights, due to changes

of wet body shape, waterline etc. Here it was assumed that the uncertainty of GMs only comes from free surface effect.

More severe free surface correction leads to less restoring. Referring to equation (2), this consequently leads to larger natural period and larger RAO amplitudes for the corresponding dof. This effect is very important, especially for dofs where their resonances are dominated by natural responses, e.g., roll motion. An example is shown in Figure 8. In addition, a free surface correction leads to an amplification of RAO amplitude at large wave period.

$$C_{44} = \rho g V \cdot GMT \quad \textbf{(10)}$$

$$C_{55} = \rho g V \cdot GML$$

Roll motion can be significantly influenced by GMT, so as to its coupled sway motion. GML correction mainly influences the pitch RAO at large wave periods. Approximately, 10% GML difference leads to about 10% difference on the pitch RAO amplitude at large periods. Considering that GML is in the magnitude of few hundred meters, free surface correction of 10% is too much. Normally free surface correction of GML is not necessary due to large stiffness in pitch dof.

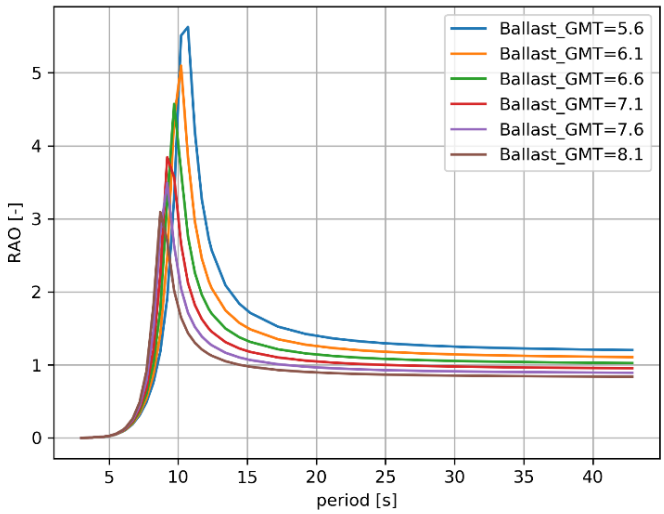

Figure 8: Roll RAO for GMT [m] sensitivity due to free surface correction, ballast condition at 90° heading, no forward speed. RAO amplitude unit in deg/deg.

Additional damping

It is well-known that there are many other types of damping in addition to potential theory related damping, for example, due to viscous effects, ref [13]. Damping plays an important role around the natural response periods. Please note that the response natural period could be different from its resonance period in the RAO. Therefore, the influence of additional damping is significant for the RAOs where the resonance is dominated by its natural response, such as roll and heave. However, it is difficult to judge how much the additional damping can be, simply due to its complexity and nonlinearity related to waves and vessel responses. Here a damping range of 0 – 16% of the critical damping for each dof at each frequency was applied, except for roll motion, where the additional damping range was assumed to be 2 – 16%.

The results show that around their resonance periods, the roll and heave RAO can be dramatically influenced by their additional damping. Also, the pitch RAO can be influenced by its additional damping, but not that significant as for roll and heave in beam sea conditions.

Numerical results

The influence of speed and water depth were considered small within their uncertainty ranges. Hence u and H were not included in the sensitivity ranking. However, speed and water depth are still important to consider when calculating RAO.

Base cases with 10kn forward speed were used. All sea states were described by long-crested Pierson Moskowitz wave spectra, with $H_S = 1m$. Tz of sea states varied from 4s to 25s with interval of 1s. and wave directions of 90˚, 120˚, 150˚, 180˚ w.r.t. the reference coordinate were considered. Each sea state was assumed 3-hour duration. The heave velocity time series were considered wide-banded and therefore, heave velocity amplitudes can be well described by the Rice distribution.

A criterion was introduced to quantify the parametric sensitivity. For each sea state, the 90-persentile value of heave velocity at the location of interest can be defined as V_{P90}^{loc}. The studied uncertainty ranges of interesting parameters are defined in Table 2. For each parameter, a number of values have been selected, and the corresponding sets of RAOs were calculated. Then for one particular parameter studied (defined as Var) and for each sea state (defined as SS), we could get several V_{P90}^{loc} values due to the variation of that parameter (values of Var defined as $\mathrm{Var(i)}, i = 1, 2, \ldots$) within the specified range. So, there will be a maximum and minimum value of V_{P90}^{loc}, defined as:

$$Vmax_{P90}^{loc}(Var, SS) = \max\{V_{P90}^{loc}(Var(i), SS)\},\ i = 1,2,\ldots \quad \textbf{(11)}$$

$$Vmin_{P90}^{loc}(Var, SS) = \min\{V_{P90}^{loc}(Var(i), SS)\},\ i = 1,2,\ldots \quad \textbf{(12)}$$

Parametric sensitivity studies of inertia terms show a weakly nonlinear effect on $V_{P90}^{loc}(Var, SS)$, while the influence from damping terms is significantly nonlinear. Here "nonlinear" means $\frac{\Delta V_{P90}^{loc}}{\Delta Var} \neq Constant$. The nonlinearity level depends on the vessel geometry, load condition, and environmental conditions such as wave direction and wave period in linear potential theory. Therefore, the difference between maximum and minimum of V_{P90}^{loc} may better indicate how sensitive the specific parameter (Var) is to RAOs and the interesting vessel response quantity within its uncertainty range, at specific location for a specific sea state, i.e., here defined as Equation (13). Alternatively, when the parameter value is close enough to the base case, $\theta_V^{loc}(Var, SS)$ defined in Equation (14) describes its parametric sensitivity near the base value, assuming that $\frac{\Delta V_{P90}^{loc}}{\Delta Var}$ is constant, for $\Delta Var \to 0$

$$Diff_V^{loc}(Var, SS) = Vmax_{P90}^{loc}(Var, SS) - Vmin_{P90}^{loc}(Var, SS) \quad (13)$$

$$\theta_V^{loc}(Var, SS) = \frac{dV_{P90}^{loc}(Var_0, SS)}{(dVar)/Var_0} \quad (14)$$

where, Var_0 is the value of Var in base case. This paper uses $Diff_V^{loc}(Var, SS)$ as the parametric sensitivity indicator.

Three locations were studied, i.e., at MRU location (loc = MRU), at crane tip starboard (loc = tip) of interest for a lift operation and at stern (loc = pip) of interest for pipelay operations. Both ballast and full loading conditions were studied. A "case" here is uniquely defined by Var, SS (H_S, T_Z, β_w), loc and loading condition. Figure 9, Figure 10 and Figure 11 show how the studied parameters affect RAOs for different sea states and locations. The oscillation noted in the figures are due to the variation of T_Z and β_w.

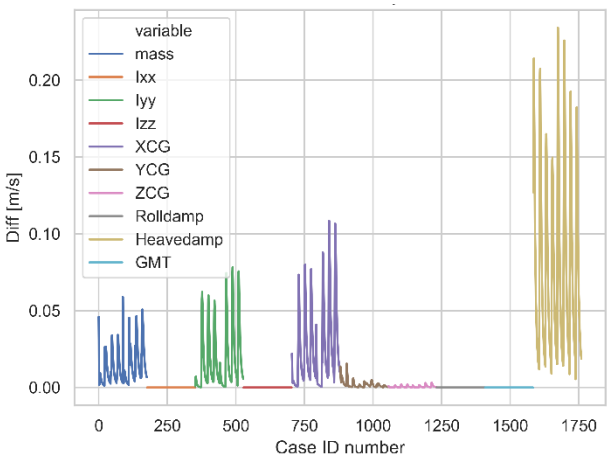

Figure 9: $Diff_V^{MRU}$ (at MRU) for all studied cases. Each Case ID number in x-axis represents a case.

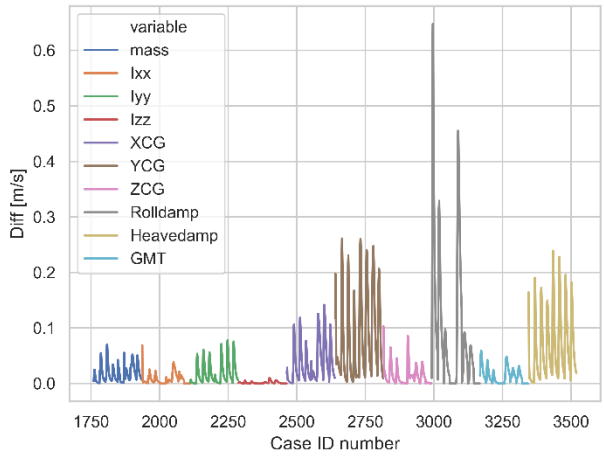

Figure 10: $Diff_V^{tip}$ (at crane tip) for all studied cases. Each Case ID number in x-axis represents a case.

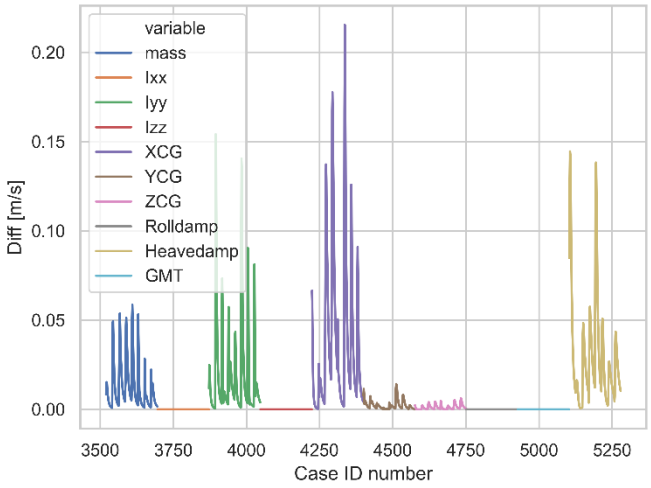

Figure 11: $Diff_V^{pip}$ (stern) for all studied cases. Each Case ID number in x-axis represents a case.

Table 3: Important parameters for RAO w.r.t. V_{P90}^{loc}

Location	Parameters
MRU	β_{33}, XCG, I_{yy}, M
Tip (crane tip)	β_{33}, β_{44}, XCG, YCG, ZCG, I_{yy}, GMT, M
Pip (stern)	XCG, I_{yy}, β_{33}, M

Table 3 summarizes the sensitive parameters for RAO w.r.t. V_{P90}^{loc} criteria for the three selected locations. The sensitivity ($Diff_V^{loc}$) for parameters listed in Table 3 are plotted on jittered polar form from Figure 12 to Figure 17 where the size of the scattered points represent the value of $Diff_V^{loc}$ for variation of Var, β_w and T_Z. Bold yellow lines separate the results for different headings. Table 4 details the heading dependent parametric sensitivity. Figures from Figure 12 to Figure 17 illustrate that the parametric sensitivity changes with T_Z and heading. One example could be for full load condition with beam sea (Figure 14). β_{33} and YCG rank first with small T_Z, while the importance of β_{44} increases with T_Z approaching resonance period. Furthermore, the sensitivity of β_{44} decreases when heading shifts towards head sea condition.

Table 4: Important parameters for RAO w.r.t. V_{P90}^{loc}, heading dependent

	MRU	tip (crane tip)	pip (stern)
90°	β_{33}, XCG	β_{33}, β_{44},YCG,GMT	β_{33}
120°	β_{33}, XCG	β_{33},β_{44},XCG,YCG, GMT	I_{yy}, XCG*
150°	β_{33}, XCG	β_{33}, XCG, YCG	XCG, I_{yy}
180°	β_{33}, XCG	β_{33}, XCG, YCG	XCG, I_{yy}

*XCG is only important for Full loading condition

The dominating parameters could change for different vessel loading conditions. For example, V_{P90}^{pip} is mostly influenced by only I_{yy} for ballast condition at 120° heading, while for full condition XCG also becomes very important.

However, this might not be the main consideration, because the uncertainty of the load condition normally will not be so large.

Please note that the conclusions in this chapter are sensitive to the selected criterion and uncertainty ranges of the considered parameters. The parametric uncertainty range may depend on vessel shape, loading condition, sensor quality, engineering experience, and etc. For example, the uncertainty studied here assumes 14% of the critical heave damping, which could be considered too much. So, in reality with reasonable uncertainty range of β_{33}, it may not show very significant influence on the interesting vessel response. Therefore, the conclusions here cannot be generalized.

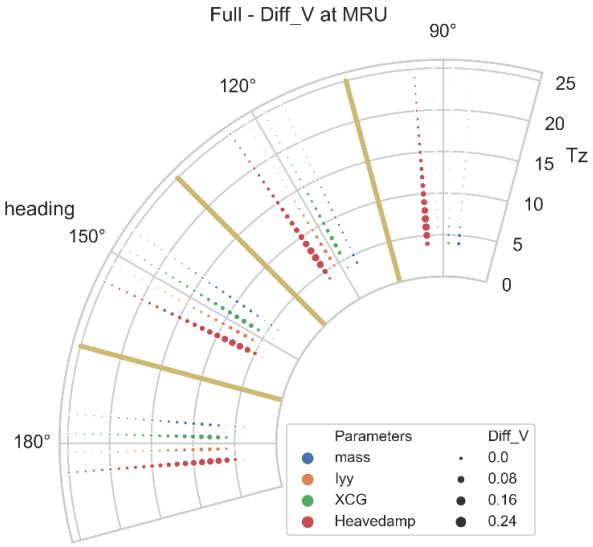

Figure 12: Jittered polar plots of $Diff_V^{MRU}$, full loading condition, for β_w= 90˚, 120˚, 150˚, 180˚, $T_Z \in [4, 25]s$

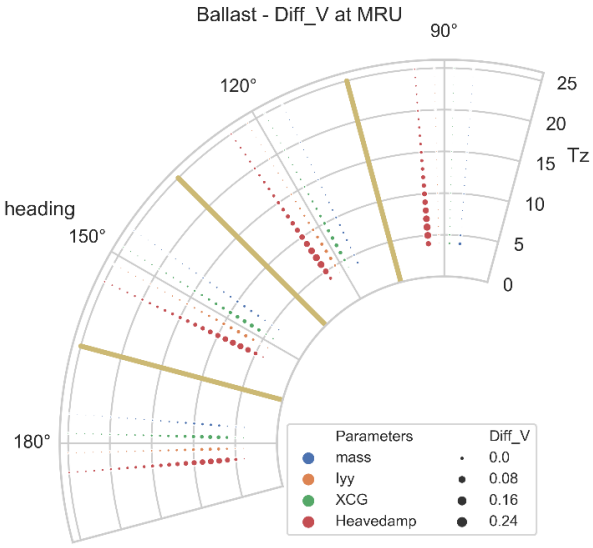

Figure 13: Jittered polar plots of $Diff_V^{MRU}$, ballast condition, for β_w= 90˚, 120˚, 150˚, 180˚, $T_Z \in [4, 25]s$

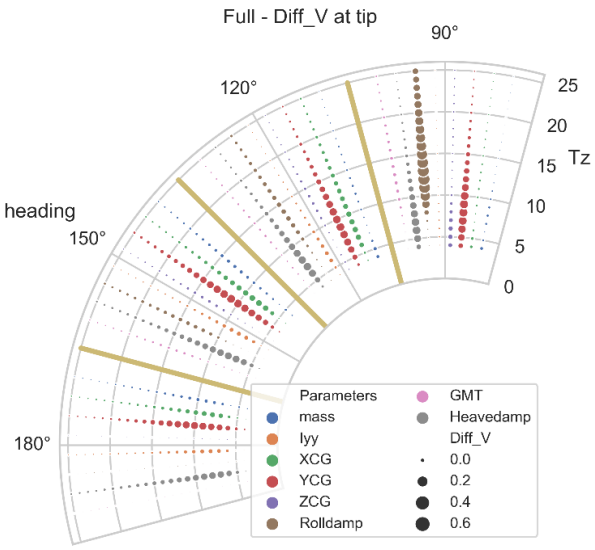

Figure 14: Jittered polar plots of $Diff_V^{tip}$, full loading condition, for β_w= 90˚, 120˚, 150˚, 180˚, $T_Z \in [4, 25]s$

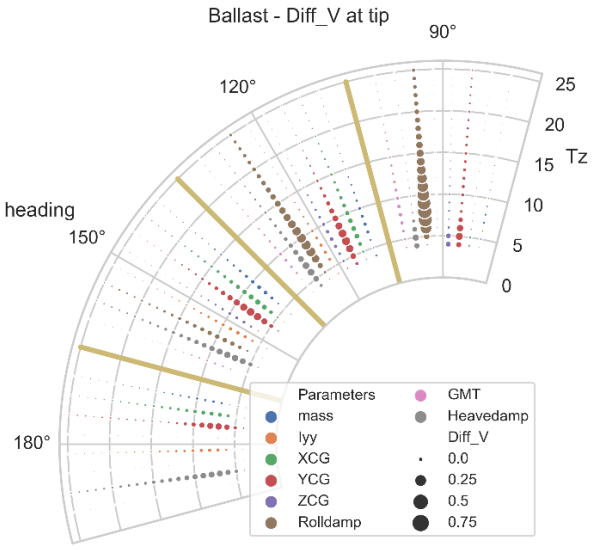

Figure 15: Jittered polar plots of $Diff_V^{tip}$, ballast condition, for β_w= 90˚, 120˚, 150˚, 180˚, $T_Z \in [4, 25]s$

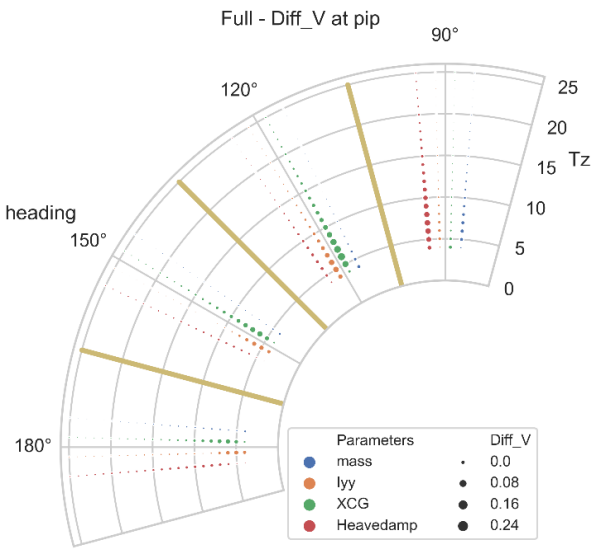

Figure 16: Jittered polar plots of $Diff_V^{pip}$, full loading condition, for β_w= 90˚, 120˚, 150˚, 180˚, $T_Z \in [4, 25]s$

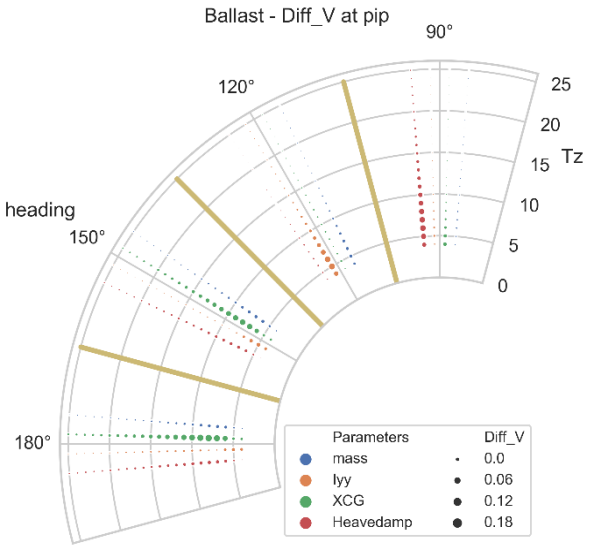

Figure 17: Jittered polar plots of $Diff_V^{pip}$, ballast condition, for β_w= 90˚, 120˚, 150˚, 180˚, $T_Z \in [4, 25]s$

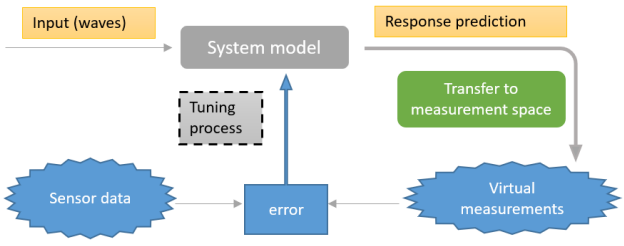

Figure 18: Example of a simple model tuning process

PARAMETER IDENTIFICATION

For digital twin application, it is essential that the numerical model can be actively adapted based on live measurements during the whole asset life time. Figure 18 shows a simple example process of system model modification. The potential applicable tuning process / methodology will not be discussed in this paper. The measurements could be, for example, the 90-percentile vertical velocity of the crane tip starboard for a duration of 3 hours where the criterion of complete tuning could be that the error of the V_{P90}^{tip} value from sensor data and prediction model is small enough, e.g., less than 10^{-4} m/s.

Assumptions and limitations

Assuming using V_{P90}^{tip} as measurement, could we succeed in tuning the hydrodynamic model to get the "right" RAO? In this paper, precise weather information and response measurements were assumed. In addition, it was also assumed that the potential linear theory perfectly describes the system except the additional damping terms. So, the only uncertainties are from the sensitive parameters of hydrodynamic model (system model in Figure 18). In this case study, it was also assumed that only one parameter was subject to modification.

The following sensor data were used, assuming no noises: 1) GPS data, so that the location, heading and speed of the vessel were known; 2) with known vessel location, weather information (e.g. sea state) could be obtained. Practically, 2D wave spectrum could be available and is considered reliable. In this study, the sea state was assumed to be perfectly described by a long-crest Pierson-Moskowitz spectrum; 3) Onboard MRU data, so the rigid body response (motion, velocity and acceleration, for all 6 dofs) at any location on vessel is known; 4) There are some sensors measuring ballast system and COG, etc. However, these measurements are subjected to uncertainties.

Case study

The sea state (SS1) and loading condition specified in Table 5 is studied, to test if we could find the right parameter for tuning in order to get the right RAO sets purely based on the criterion of the V_{P90}^{tip}:

Table 5: Study case information – SS1

Parameters	Value
H_S	2 m
T_Z	10 s
β_w	120 ˚
Loading condition	Ballast (approximately)

According to conclusion from Table 4 and to limit the scope, XCG, GMT and β_{44} were considered as candidate parameters for tuning in this case study. The 3-hour V_{P90}^{tip} at (60.0, 13.0, 12.0) w.r.t. the reference coordinate system, was set as criterion for model tuning. Tuning process was considered complete whenever the error of V_{P90}^{tip} was less than 10^{-2} m/s.

Applying the presumed base model (i.e. ballast condition, deep water, 10kn, with 5% additional roll damping and -0.5m GMT correction), $V_{P90}^{tip}(base\ model, SS1)$ is 1.31 m/s. Then the measurement $V_{P90}^{tip}(Var, SS1)$ of 1.29 m/s is received. The true parameter to tune from the base case of ballast condition is actually GMT from -0.5m to -0.25m. However, all the following 3 tuning results will meet the P90 criterion:

1. Case A: correction of XCG 1.0m towards stern
2. Case B: correction of β_{44} from 5% to 5.5%
3. Case C (True case): GMT free surface correction from -0.5m to -0.25m

Figure 19 shows the RAO of Heave velocity at the crane tip from Case A, B and C. Please note that the "true" model is actually quite close to the presumed base model. So, it may not expect large difference of heave velocity RAO among Case A, B and C. However, clear difference of crane tip heave velocity RAO is seen at response periods from 8s to 14s.

T_P of SS1 is about 14s for PM spectrum, ref [21]. At this peak period, there is insignificant RAO difference. However, if the tuned model from Case A or Case B is used, errors of future response predictions for sea states with T_P between 8s and 14s may be expected.

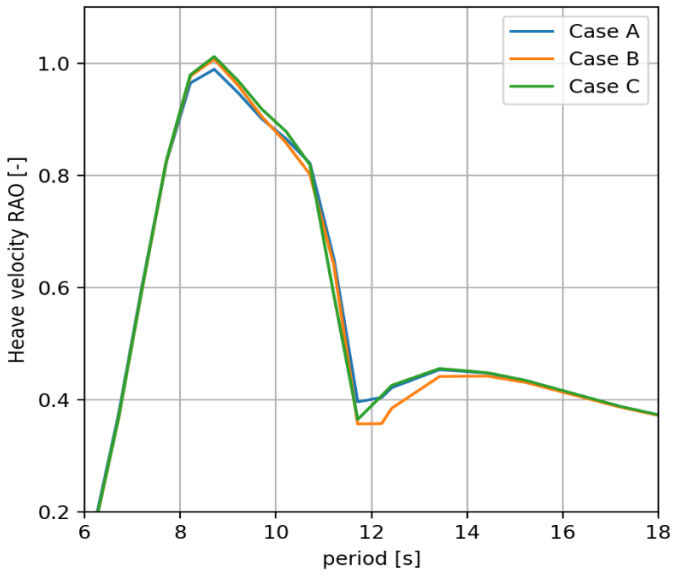

Figure 19: Heave Velocity RAO at crane tip, 120˚ wave heading.

From this case study, it can be concluded that it is not possible to identify the true parameter for tuning, only based on one criterion and one sea state measurement. Consequently, it would also be difficult to estimate how much the error could be due to using the tuned RAO from a wrong parameter.

Measurements from more sea states

Can the correct parameter be identified to tune by using more measurements from different sea states? In addition to measured V_{P90}^{tip} from SS1, measurement from another sea state, SS2 ($H_S = 3m$, $T_Z = 7$s, $\beta_w = 120^\circ$), is available. $V_{P90}^{tip}(base\ model, SS2) = 2.34\ m/s$. The measured V_{P90}^{tip} for SS2 is 2.32 m/s.

Table 6: Tuning results (from base case) – measurements from two sea states

Parameters	SS1	SS2
XCG	-1.0m	-0.4m
β_{44}	+0.5%	+0.37%
GMT	**+0.25m**	**+0.25m**

Results in Table 6 show that only the tuning of GMT agrees perfectly between SS1 and SS2. Therefore, confidence is increased to exclude XCG from the three tuning candidates. However, one still cannot exclude β_{44} as a tuning candidate, because the additional roll damping is sea state dependent. This means that sea state dependent parameters cannot be identified by getting more measurement from other sea states. So, for model tuning, it is valuable to split the candidate parameters into categories of permanent, loading condition dependent and sea state dependent.

More criteria

As has been shown, different parameters influence the RAOs in different ways. Some parameters mainly influence RAO at a limited range of period (e.g., additional damping) and for some specific dofs (e.g., GMT). Some parameters only affect the amplitude of RAO (e.g. additional damping), while some parameters can affect both amplitude and peak period of RAO (e.g. GMT, XCG). It could be important to take these properties into account when identifying the right parameter to tune.

Vessel response at a specific location may contain vessel RAO information for multiple dofs. For example, heave motion at crane tip results from heave, roll and pitch motion RAO at midship. Different criteria, e.g., using measurements from other locations, V_{P90}^{locj}, may help to identify the right parameter to tune. In addition, the derivatives and integration of the velocity RAOs could also give more useful information. This means, applying motion and acceleration responses as additional criteria may help to identify the right parameters to tune.

SS1 is again used for case studies. Candidate parameters are still XCG, GMT and β_{44}. Case study "Locations" uses the P90 heave velocity for SS1 at two different locations, i.e., crane tip starboard (tip) and stern 10m starboard from vessel longitudinal axis (st10). Case study "Response" uses the P90 heave acceleration for SS1 at tip location, $A_{P90}^{tip}(SS1)$, in addition to $V_{P90}^{tip}(SS1)$.

Results in Table 7 and Table 8 show that multiple criteria for one sea state help exclude both loading condition dependent and sea state dependent parameters, promisingly leading to identify the right parameter for model tuning. Using different responses at the same location might be a better choice compared with same response type at different locations. Because response at

different locations is calculated based on rigid body motion assumption, which could be challenging for large vessels.

Table 7: Tuning results (from base case) – Case "Location"

Parameters	tip	st10
XCG	-1.0m	-1.37m
$\boldsymbol{\beta_{44}}$	+0.5%	-0.25%
GMT	**+0.25m**	**+0.25m**

Table 8: Tuning results (from base case) – Case "Response"

Parameters	V_{P90}^{tip}	A_{P90}^{tip}
XCG	-1.0m	-0.68m
$\boldsymbol{\beta_{44}}$	+0.5%	+0.3%
GMT	**+0.25m**	**+0.25m**

CONCLUSION AND DISCUSSION

It is important to consider the effects from water depth and vessel speed when building RAO functions. However, considering the uncertainty of the vessel speed and water depth measurements, and considering the simplifications of the applied theories for hydrodynamic analysis regarding vessel speed and shallow water effects, it might not be necessary to include those parameters for tuning purpose. When building RAO database, it is suggested to have sufficient resolution of water depths and vessel speeds to ensure the accuracy of RAO sets for the future use. Validation of potential theory could be challenging for very shallow water depth and uneven seabed conditions.

Ignoring the weak nonlinearity of parametric sensitivity to RAOs discussed in "Numerical results" section, the uncertainty of most interesting parameters could be well described by a Gaussian model, with the prior value representing the most probable (mean) value. However, for modelling uncertainty of additional damping, this might be questionable, because 1) biased engineering judgement usually is applied; 2) and the uncertainty is usually not symmetric w.r.t. the prior damping value used.

This paper describes how the selected vessel hydrodynamic model parameters affect response RAOs. Parametric sensitivity to RAOs depends on T_Z, β_w, location, load condition and corresponding parametric uncertainty range, etc. The study shows that β_{33}, β_{44}, COG, I_{yy}, GMT and M are important parameters with respect to the vessel response sensitivity, and therefore could be selected for model tuning.

Model tuning requires to identify the correct parameter(s) first. The case study for parameter identification shows that measurements from different sea states cannot help identifying sea state dependent parameters. It is valuable to apply multiple criteria and multiple types of measurements (e.g., different locations and responses) to identify the correct parameter. The case study on parameter identification assumed precise knowledge on weather information and vessel response measurements, and only one parameter was subject to model tuning. However, real world is noisy and uncertain. The number of tuning parameters is normally also unknown. In addition, there is an uncertainty due to model simplification of vessel response system in potential theory. These uncertainties can lead to potentially overfitting or underfitting problems. Future work is required on how to identify multiple parameters for tuning process. In reality, no candidate parameters can be excluded due to uncertainties and noises from input and measurements. However, this can hopefully be circumvented by probabilistic modelling of candidate parameters.

ACKNOWLEDGEMENTS

This work was made possible through the Centre for Research based Innovation MOVE, financially supported by the Norwegian Research Council, NFR project no. 237929 and the consortium partners, http://www.ntnu.edu/move. Special thanks are given to Olav Rognebakke, Jens Bloch Helmers, Håvard Nordtveit Austefjord and Hui Sun in Section of Hydrodynamics & Stability in DNV GL for providing models, and various helpful technical discussions and supports. Thanks are also given to DNV GL Riser Technology Section for providing office and facilities when the first author studied at Høvik.

REFERENCES

[1] O. Faltinsen, "Sea Loads on Ships and Offshore Structures," Cambridge University Press, 1993.

[2] L. K. Alford, R. F. Beck, J. T. Johnson, D. Lyzenga, O. Nwogu og A. Zundel, «A Real-time System for Forecasting Extreme Waves and Vessel Motions,» i *OMAE*, 2015.

[3] B. Connell, J. Rudzinsky og C. Brundick, «Development of an environmental and ship motion forecasting system,» i *OMAE*, St. John's, 2015.

[4] J. Kusters, K. Cockrell, B. Connell, J. Rudzinsky og V. Vinciullo, «FutureWavesTM: a Real-time Ship Motion Forecasting SYstem employing Advanced Wave-Sensing Radar,» i *IEEE*, 2016.

[5] G. F. Clauss, S. Kosleck og D. Testa, «Critical Situations of Vessel Operations in Short Crested Seas - Forecast and Decision Support System,» *Journal of OMAE,* vol. 134, 2012.

[6] J. Dannenberg, K. Hessner, P. Naaijen, H. Boom og K. Reichert, «The On Board Wave and Motion Estimator OWME,» i *ISOPE*, Beijing, 2011.

[7] G. Clauss, S. Kosleck, D. Testa og K. Hessner, «Forecast of critical situations in short-crested seas,» i *OMAE*, Estoril, 2008.

[8] P. Naaijen, D. Roozen og R. Huijsmans, «Reducing operational risks by on-board phase resolved prediction of wave induced ship motions,» i *OMAE*, Busan, 2016.

[9] J. Nielsen, N. Pedersen, J. Michelsen, U. Nielsen, J. Baatrup, J. Jensen og E. Petersen, «SeaSense - Realtime Onboard Decision Support,» WMTC, 2006.

[10] E. A. Tannuri, J. V. Sparano, A. N. Simos and J. J. D. Cruz, "Estimating directional wave spectrum based on stationary ship motion measurements," *Applied Ocean Research,* vol. 25, pp. 243-261, 2003.

[11] U. D. Nielsen, A. H. Brodtkorb and A. J. Sørensen, "A brute-force spectral approach for wave estimation using measured vessel motions," *Marine Structures,* pp. 101-121, 2018.

[12] W. Qiu, J. Junior, D. Lee, H. Lie, V. Magarovskii, T. Mikami, J. Rousset, S. Sphaier, L. Tao and X. Wang, "Uncertainties related to predictions of loads and responses for ocean and offshore structures," *Ocean Engineering,* vol. 86, pp. 58-67, 2014.

[13] ITTC, "ITTC Quality System Manual Recommended Procedures and Guidelines - Numerical Estimation of Roll Damping," 2011.

[14] «Wasim User Manual,» DNV GL, 2018.

[15] D. Kring, «Time Domain Ship Motions by a Three-Dimensional Rankine Panel Method,» 1988.

[16] Y. Luo, «Numerical Investigation of Wave-Body Interactions in Shallow Water,» NTNU, 2013.

[17] U. D. Nielsen, «Transformation of a wave energy spectrum from encounter toabsolute domain when observing from an advancing ship,» *Applied Ocean Research,* vol. 69, pp. 160-172, 2017.

[18] G. Clauss, F. Stempinski, M. Dudek and M. Klein, "Water depth influence on wave-structure-interaction," *Ocean Engineering,* vol. 36, pp. 1396-1403, 2009.

[19] K. McTaggart, «Ship Radiation and Diffraction Forces at Moderate Forward Speed,» 2015.

[20] J. Journee og J. Pinkster, Introduction in Ship Hydromechanics, Lecture MT519, 2002.

[21] "DNVGL-RP-C205 Environmental conditions and environmental loads," DNV GL, 2017.